Available online at www.sciencedirect.com

ScienceDirect

Procedia Engineering 2 (2010) 2219–2227

Procedia Engineering

www.elsevier.com/locate/procedia

Fatigue 2010

Digital Image Correlation technique: application to early fatigue damage detection in stainless steel

Marion Risbet[a*], Pierre Feissel[a], Thierry Roland[b], Delphine Brancherie[a], Jean-Marc Roelandt[a]

Université de Technologie de Compiègne, Centre de Recherches de Royallieu, 60200 Compiègne, France
Institut National des Sciences Appliquées, 24 Bld de la Victoire 67084 Strasbourg, France

Received 4 March 2010; revised 12 March 2010; accepted 15 March 2010

Abstract

In the context of development of a numerical model, to accurately predict the fatigue life of a structural component, it is fundamental to consider both the initiation stage and the propagation stage of micro-cracks. Such a development requires dedicated experimental tools both to provide the physical understanding needed for designing models and to validate the proposed approaches and models. Thus, this paper presents the experimental means that need to be used for such a purpose. The approach is based on the analysis of displacement field measurements by digital image correlation (DIC) during low-cycle fatigue tests. A specific filtering tool is also presented to minimize the committed errors when derivative operation is performed for strain calculation. Therefore, in this quite recent application of DIC, the reproducibility of the method has to be questioned and validated, with help of some more conventional strain measurements devices. It seems that the experimental conditions have to be carefully controlled, so that the results can be interpreted in terms of mechanical phenomena.

Keywords: Digital Image Correlation; mechanical tests; low-cycle fatigue, damage initiation; stainless steel

1. Introduction

The prediction of the lifetime of a mechanical structure from the conception stage remains a main industrial matter. When basing the conception on damage tolerance, the behaviour of a structure taking defects and cracks into account is to be studied from a numerical point of view in order to describe the physics of the phenomena properly. The most usual studies of lifetime prediction take the propagation phase of the cracks into account, while neglecting the initiation, leading to the underestimating of the total lifetime. In order to improve this point, both initiation and propagation stages are to be mastered; this would allow a more accurate estimation of the safety of cracks and hence

*Corresponding author *:E-mail address*: marion.risbet@utc.fr

1877-7058
doi:10.1016/j.proeng.2010.03.238

help define control processes, in order to plan repairs while ensuring security, cost-effectiveness and environment care.

Nonetheless, a few tools are able to manage both initiation and crack propagation, since the models dedicated to each phase are very different. The crack propagation description is often based on the linear or non-linear fracture mechanics and can be implemented through various numerical approaches (e.g. boundary elements, X-FEM).

Notwithstanding, such methods do not suit to the description of initiation and short cracks propagation stages. A local analysis at the volume element scale is then required, and the modeling based on damage mechanics seems more pertinent to this context. A main drawback in using these methods in computation is the pathological mesh-dependency of the solution. The use of the strong discontinuity approach [1] tackles this problem and allows an objective description of the cracks initiation. The modeling of the damage of the representative volume element is then performed from the first localization zone up to the creation of a macrocrack that will lead to the final rupture of the structure.

The present work is a part of a global study, which aims to propose a numerical modeling strategy of rupture from initiation to propagation, for a structure under cyclic loading. Such an approach needs the development of models based on a close understanding of the physics from experimental observations. These observations are of tremendous importance and have to comply with various complementary goals: allowing an early and robust detection of the initiation of cracks taking the heterogeneity of the material at the grain scale into account, tracking the propagation of cracks and helping construct quantitative criteria for the models through quantitative measurements (e.g. crack length, local strain and energy). All these reasons led us to propose a specific experimental strategy whose purpose is to optically track the surface of the specimen during cyclic loading at the grain scale. The objectives and first results of the proposed approach are first presented. The snapshots taken during the test are treated through Digital Image Correlation [2], yielding the displacement fields. A dedicated method, based on space-time diffuse approximation, is proposed in order to reconstruct the strain field from the measured displacements, aiming at controlling the errors on the reconstruction. The method is finally applied to several specimens enduring a low-cycle fatigue test in the same experimental conditions. It seems that many parameters are to be controlled, and that performing this type of test enhances many questions about the reproducibility of the experimental tests.

2. Experimental section

2.1. Material

The chosen material is an austenitic stainless steel 316L with a FCC structure, with an elastic limit of 280 MPa. The austenitic stainless steel that is studied here has low stacking fault energy (SFE~25mJ.m^{-2}). It tends to develop plasticity through persistent shear bands (PSB) and twinning whose magnitude depends on the strain rate and strain level. In fatigue, the damage mechanisms remain mainly influenced by the level of the loading. Henz and Neumann [3] studied the effect of the twin boundaries on the crack initiation for high-cycle fatigue. With a low level of the loading, some PSBs may develop along the twin boundaries and their plastic activity can lead to early crack initiation. Some modeling of these phenomena has been proposed, e.g. Henz and Neumann [3] or Essmann, Gosele and Mughrabi [4]. For larger strain magnitude, the crack initiation locations depend drastically on the texture of the material and the meso-texture of the specimen. Once the microcrack has appeared on the twin boundaries, it propagates in a trans-crystalline manner [5]. The mean grain size is here about 60 μm. The crystallographic texture could not be analyzed, but it will be done in the future.

2.2. Mechanical tests

The specimens are stamped from a 2 mm thick laminated plate in the rolling direction. Figure 1(a) presents the flat specimen geometry that has been chosen in order to concentrate the stresses in a 4x3 mm^2 local zone around the middle of the specimen. This should allow the study of crack initiation and propagation in this zone. The tests are performed on an Instron servo-hydraulic machine (maximal force 25kN), at ambient temperature. Traction-traction

cycles from 60 MPa to 600 MPa (R=0.1) are applied to the specimen at a test frequency about 15Hz until total fracture. The maximum load is about 90% of the rupture load, it corresponds to low-cycle fatigue conditions. These mechanical conditions have been applied for the three specimens tested in the present paper.

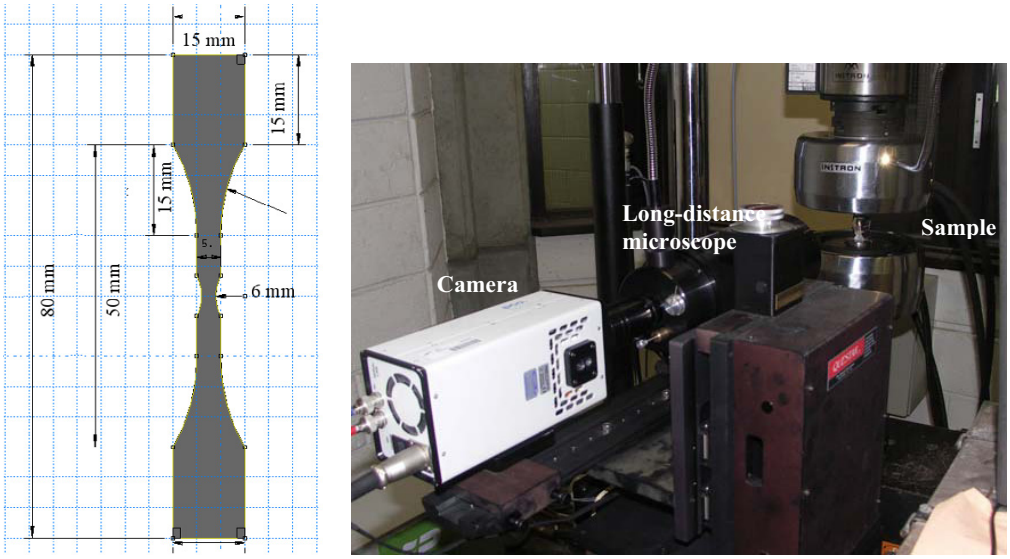

(a) (b)

Figure 1. (a) Geometry of the flat specimens and (b) experimental set-up

2.3. In situ optical analysis and sample surface preparation

One of the key points of the experimental study is to perform an optical tracking of the damage during the fatigue test at a fine enough scale in order to characterize the initiation of cracks. It is based on Digital Image Correlation (DIC) so that one will be able to reconstruct the displacement field on the studied zone. Such data is much richer than the one yielded by standard gauges and it is therefore expected to provide some information on the local phenomena.

The DIC tools, such as Correli-Q4 [2] that is used here, are more effective when the images are made of random patterns. At the macroscopic level, one can use painting in order to add an artificial speckle to the surface of the specimen. Such approach is not suited when studying finer scales, since the size of the speckle is of the same order as the grain size [6]. Furthermore, the use of painting may influence the surface properties of the specimen, who play a major role for crack initiation. It is possible to improve the texture of the specimen through several techniques, in order to have a micro-speckle, e.g nanoparticles [6] or chemical or physical deposition (CVD and PVD) [7]. In our case, we can afford to base the DIC on the natural texture of the specimen's grains, which is revealed by electropolishing. Specimen gauge length was then electropolished in a 10%w oxalic acid solution during 50 s with a voltage of 10V (I=0,6A).

Since we are interested in the grain scale, one has to use DIC with a set up allowing a large magnification of the specimen. To that purpose, several tools can be used, as for instance an atomic force microscope [8] or a scanning electron microscope [9], allowing a good accuracy on the measurement. With a resolution of 0.179µm, an error on the displacement of 0.026 pixels can be achieved. Nonetheless, these tools are not suited for *in situ* tracking on a standard tensile or fatigue test. From [11-13], it was shown that the use of an optical microscope might be

appropriate for the tracking of damage at the grain scale on a stainless steel such as the 316L. A long range microscope Questar QM100 allows a spatial resolution of 0.6 µm at a working distance of 23.1 cm, yielding to 800x600 μm^2 zones of interest. It is mounted on a translation stage allowing a tracking of the studied zone all along the test. The Questar QM100 is used coupled with a 12-bit CCD camera. A picture of the experimental set-up can be found in figure 1(b).

It has been chosen to take snapshots during the test at the maximum load all along the test. The frequency of the snapshot has been adapted depending on the specimen, and on the phase of the test, as it will be detailed in section 4.

The displacement and the deduced strain reconstructed from DIC will therefore be with a reference frame taken at the first cycle at maximum load. The studied displacement and strain will be denoted as an additional strain when compared to the total strain from the unloaded state at the beginning of the test. This additional strain is equal to zero when nothing occurs between the reference cycle and the cycle where the strain is estimated and should give rich information on local phenomena occurring such as cracks development. The main difficulty with this quantity is that it is very sensitive to noise on the measurement, since its magnitude is of 0.1% while the total strain is about 30%. It is therefore important to reconstruct the strain field from the displacement field with great care and this led us to develop a specific space-time filtering tool based on diffuse approximation which is presented in the following.

3. Strain reconstruction through diffuse approximation

3.1. Need of a filtering

As mentioned in Section 2, the fatigue tests performed in this study are coupled with an optical measurement allowing the use of Digital Image Correlation at fine scales. The snapshots are treated through the CorreliQ4 [2] algorithm in order to reconstruct the additional displacements on a zone where the cracks are expected to initiate. The displacement field is of interest once the macrocracking has appeared, since the latter corresponds to a displacement jump, but, before the crack propagation, the initiation may be better tracked by the strain field. It is therefore expected to reconstruct the strain field from the measured displacement field, through its numerical differentiation.

Such an operation is very sensitive to the measurement random error and this difficulty has to be tackled. In [10], a filtering method based on the Diffuse Approximation [11] was proposed. The results on simulated and experimental data demonstrated the ability of the method to reconstruct the strain field while controlling the reconstruction error. The effectiveness of the filtering is tuned by the radius of influence of the measurement points, which controls both the random error and the approximation error on the strain field. A compromise has to be found between these two types of error, a larger radius leading smaller random error but larger approximation error. Since the fatigue test yields a large amount of snapshots (from 500 to 1000 in the treated examples here), the idea is to take advantage of it by filtering several snapshots at one time, instead of one snapshot after another. The evolution along the time will therefore be taken into account and it should allow reducing the space radius, hence keeping the same filtering while decreasing the approximation error.

3.2. Space-time diffuse approximation

For each snapshot, the displacement data are known on a regular grid of data points in space. Each data grid corresponding to a given time, they are stacked together so that a 3D time-space data grid is constructed. The displacement data are therefore given on N points, denoted M_{ij} with coordinates (x_i,t_j) stored in two vectors: $\{U_{exp}\}$ and $\{V_{exp}\}$, corresponding to the longitudinal and transversal coordinates of the displacement. From this 3D data grid, one aims at reconstructing the two continuous displacement fields U(x,y,t) and V(x,y,t) and their gradients at any point X = (x ,t) from $\{U_{exp}\}$ and $\{V_{exp}\}$. The proposed approach is based on the use of local weighted least squares and the local regression tool is the Diffuse Approximation [11]. The filtering parameter is the radius of influence of each data point, which will be defined independently in space and time and respectively denoted R_x and

R_t. Such an approach provides at once the displacement field and its derivatives in diffuse manner. The reconstructed field is seek at any X = (x ,t) as the solution of the following minimization:

$$\min_{a(\underline{x},t)} \frac{1}{2} \left(P\{a\} - \widetilde{U}\right)^T W \left(P\{a\} - \widetilde{U}\right) \quad \text{avec,} \quad P = \begin{bmatrix} p(\underline{X}_1 - \underline{X}) \\ \dots \\ p(\underline{X}_N - \underline{X}) \end{bmatrix}_{i \in V(\underline{X})} \tag{1}$$

p(X) is a line vector who collects the functions of the approximation basis, not necessarily polynomial . The choice here is to use a degree 2 polynomial basis (10 monomials in space and time 3D). When dealing with standard space Diffuse Approximation, this choice appeared to be in [10] a good compromise between mechanical approximation and filtering. With such a basis, the terms $a_2(X)$ and $a_3(X)$ are estimates of the first spatial derivatives of the displacement field at point X, in a diffuse manner. V(X) is the neighbourhood of X who collects the measurement points contributing to the reconstruction at point X and its size is directly related to (R_x,R_t). The matrix W is a diagonal matrix made up of the weighting functions $w(X,X_i)$ and ensures the continuity of the reconstructed field. The minimization problem (1) leads to a linear problem that can be solved for any X. Here, it is chosen to evaluate the reconstructed field at the data points, that is for any $X = X_{ij}$.

3.3. Filtering of the measurement random error

When filtering the displacement measurements, the increase of the span of the weighting function improves the filtering but may imply a large approximation error. The idea was hence to introduce a filtering in both space and time at once. The aim here is therefore to compare the filtering effectiveness of this new space-time filtering with respect to the filtering of the standard space Diffuse Approximation [10]. Assuming the random error {δu} on the displacement measurements is modeled by a centered Gaussian white noise whose standard deviation is denoted σ_b, it is possible to estimate the standard deviation on the reconstructed strain field $\delta\varepsilon_b$, who is also a Gaussian variable. Denoting M_ε the linear strain reconstruction operator, the standard deviation comes from:

$$cov(\delta\epsilon_b) = \left\langle \delta\epsilon_b \delta\epsilon_b^T \right\rangle = \left\langle M_\epsilon \{\delta u\} \{\delta u\}^T M_\epsilon^T \right\rangle = {\sigma_b}^2 M_\epsilon M_\epsilon^T \tag{2}$$

In the case where the assumption of a white noise on the measurement is not reasonable but the covariance matrix of the random error is known, like in [2], the latter can be taken into account in equation (2).

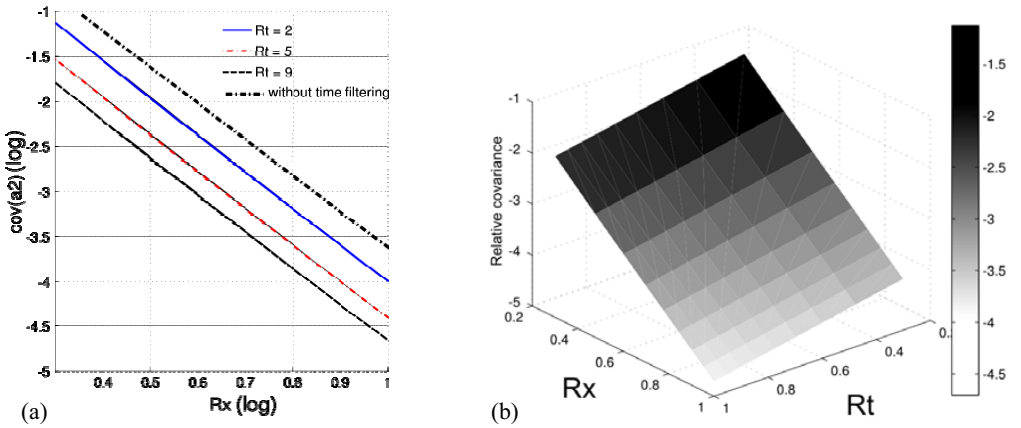

Figure 2 Standard deviation as a function of the filtering parameters (σ_b = 1) (a) curves with given time radius (b) curves with given space radius

Figure 2 presents the variance on the reconstructed first derivative of the displacement as a function of the filtering parameters, in a log scale, for an input random noise with unit standard deviation. Figure 2-(a) compares the filtering as a function of the space radius for various time radii. It is shown that a time radius increase improves the filtering for a given space radius. As a consequence, for a given filtering level, one can reduce the value of the space radius when increasing the time radius, and hence reduce the approximation error. Figure 2-(b) presents the evolution of the filtering as a function of both the space and the time radii. One can note the filtering slope is smaller with respect to R_t than to R_x.

From these statements, it is possible to deduce curves such as those presented on Figure 3, each corresponding to a level of filtering of the random error. With these isofiltering curves, it is then possible to choose a couple (R_x,R_t) allowing a given level of filtering while choosing the best compromise with the approximation error.

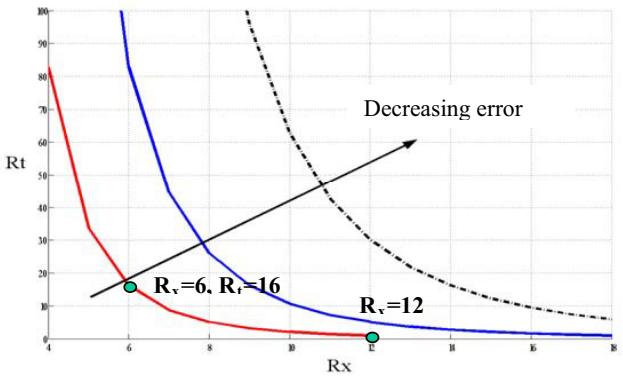

Figure 3 Isofiltering curves in the (R_x,R_t) plan

4. Application to low-cycle fatigue tests

In this last part, we present a first application of the space-time filtering on a fatigue test. The test was performed on three 316L stainless steel specimens as presented in Section 2.2.

4.1. Frequency of snapshot during the tests

In order to track the local evolution along the cycles, snapshots are taken at maximum loading, yielding from 500 to 1000 pictures. A first specimen (S1) was tested, with a frequency of snapshot kept constant throughout the tests (every 60 mechanical cycles). Then, using CorreliQ4, a Digital Image Correlation tool [2], the displacement field is reconstructed between each snapshot and the reference one, corresponding to the tenth cycle at maximum load. The reconstructed displacement is therefore an additional displacement. It may be appropriate for the detection of local phenomena, but its drawback is its sensitivity to the noise, which is emphasized when reconstructing the associated strain. The spatial mean of this additional strain is represented on Figure 4 as a function of the cycle number until fracture. One can observe that this strain magnitude remains rather small, about 0.15%, compared to the total plastic deformation (30%), evaluated from the tension curve. On Figure 4, three phases of the test can be observed corresponding to three different additional strain rates. The dashed line corresponds to the strain filtered through space-time diffuse approximation. For the following specimens, it was decided to increase the number of pictures in the first 5000 cycles of fatigue, where the additional strain has a greater variation. During the two following tests, one picture every 15 mechanical cycles has been taken to that aim. As a remark, it represents a great implication of

two operators all along the fatigue test, since the camera acquisition is not automatically synchronized with the testing machine yet.

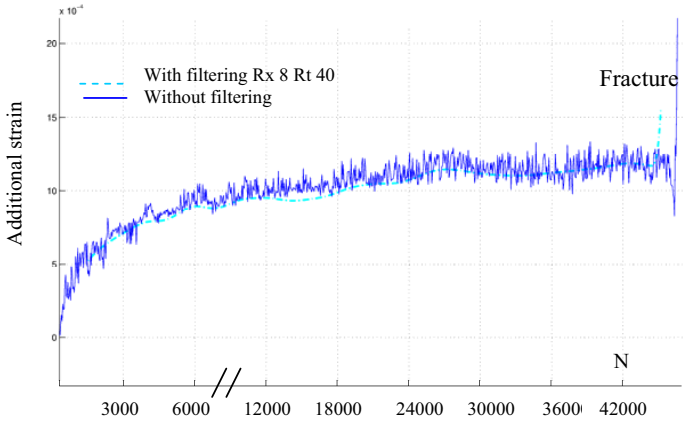

Figure 4. Evolution of the additional strain with the number of cycles N for specimen S1 with and without filtering.

4.2. Crack initiation observation

Although the first test was conducted until the total fracture of S1, which occurred at 45.000 cycles, no crack initiation was detected in the interest zone through the long distance microscope observations. As a consequence, for the following tests on specimens S2 and S3, we made slight modifications of the surface sample preparation, by taking care of preparing similarly both sides of the flat specimen for instance, since damage initiated on the other specimen side. This was not sufficient to induce crack initiation in the zone of observation. We are currently working on the modification of the specimen geometry, because the present design fails in localizing the crack deformation in a sufficient way according to the reduced size of the interest zone. From a general point of view, working in a very local scale induces the risk of missing the crack initiation occurring in another part of the specimen. To help finding the number of cycles for crack initiation, some acoustic emission tracking is intended to be added to these optical measurements.

4.3. Additional strain evolution and level of noise

Figure 5(a) presents the evolution of the additional strain restricted to the first 5000 cycles for the 3 specimens. As the specimen S3 was also equipped with an extensometer, it was possible to calculate an additional strain by subtracting the value of the strain at maximum load for the 10^{th} cycle to the ones for the other cycles, at the global scale. The results are given in Figure 5(b).

We can first remark that the level of additional strain is of the same order between the two methods for S3, below 1.10^{-3}, even if the "optical" strain is quite smaller than expected with the extensometer. The evolution with N is similar too, indicating a ratcheting phenomenon in both cases. It is worth noting that a very local zone of observation (800 µm x 600 µm) can be used as a virtual strain gauge as well as an extensometer with a 25 mm gauge length. This zone can also be considered as an elementary representative volume, suitable for further analysis.

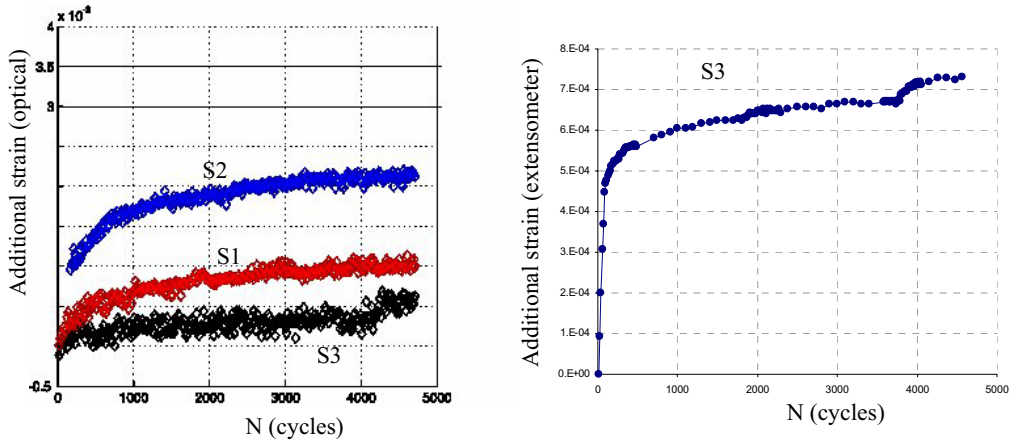

(a) (b)

Figure 5 (a) Additional strain versus N, number of cycles for specimens S1, S2 and S3, obtained with picture analysis – (b) Additional strain versus N, number of cycles, calculated for specimen S3 from extensometer data.

This strain ratcheting is a characteristic of the three specimens, as seen in Figure 5(a). Nevertheless, neither the level of additional strain nor the number of cycles needed to obtain the additional strain saturation is reproducible from one specimen to another. These differences are difficult to analyze because of the lack of information for S1 and S2, these tests being not instrumented with an extensometer. In particular, are these differences representative of a difference of mechanical behaviour between the specimens, or are they linked to a varying quality of the optical local information?

To go further in that way, Figure 6 presents an example of the additional displacement field for two different cycles in the last 1000 cycles before fracture (where the additional strain level is the highest), in case of specimen S1.

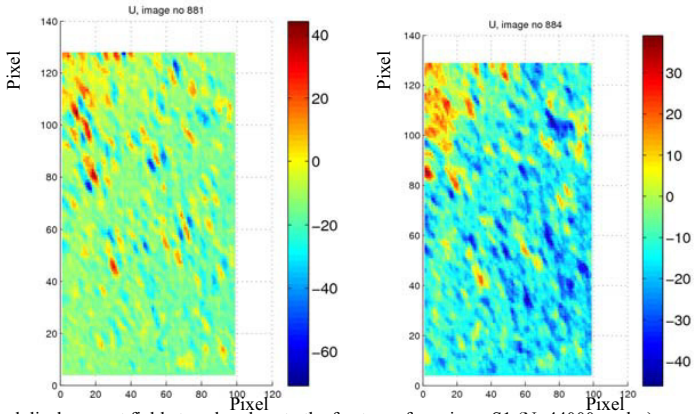

Figure 6 Additional displacement field at cycles close to the fracture of specimen S1 (N~44000 cycles).

Unfortunately, the level of noise prevents from reconstructing reasonable strain fields, even with the help of the filtering tool presented in section 3. This drawback is common for the additional strain fields obtained for the three specimens tested in this study whatever the number of cycles. This could mean that the mechanical strain field has no heterogeneities at this scale, which is perhaps too wide to access the intergranular strain incompatibilities that may be created during the cyclic test. But this hypothesis is linked to the absolute value of the level of noise, which must not be too high to highlight the purely mechanical information.

Consequently, these first results are not sufficient to conclude, and moreover they induce many questions. Therefore, more tests have to be done to validate the experimental procedure, and to know exactly what is optically measured during the test. A particular effort has to be done to reduce the level of noise. Several ways of improvement are planned, for instance by improving the quality of the lighting on the observed zone. We are presently working on the automatic synchronization of the testing machine with the camera, so that a larger database of tests can be easily achieved.

5. Conclusion

In this paper, we presented the first steps of an experimental approach dedicated to the study the local phenomena occurring during a fatigue test. A filtering tool based on space-time diffuse approximation was proposed and applied to the tests yielding encouraging results. The experimental study has to be continued through new fatigue tests in order to reach the local information which is expected. Some modifications have to be made in the experimental procedure to localize the damage in the observed zone, and to improve the quality of the pictures. The optically measured local information has to be compared to the global information obtained by more classical strain measurements devices, in order to get a correct interpretation of the phenomena. The discrimination between noise level and mechanical information is the key point of the whole framework. Then, this information is intended to be used to develop a numerical modeling of the fatigue rupture, from initiation to propagation of cracks.

Acknowledgements

The authors would like to thank the Regional Council of Picardie for its financial support on this study. Many thanks to our technical staff, Gérard Marichal for performing the mechanical tests, and Jean-Patrick Wtyklo for SEM observations.

References

[1] D. Brancherie, A. Ibrahimbegovic, Novel anisotropic continuum-discrete damage model capable of representing localized failure of massive structures. part I : theoretical formulation and numerical implementation. *Engineering Computations*, **26** (1-2),100-127, 2009.
[2] G. Besnard, F. Hild, S. Roux. “Finite-element” displacement fields analysis from digital images : application to Portevin-Le Châtelier bands. *Expl Mechanics*, 46 (6) 789–804, 2006.
[3] A. Heinz, P. Neumann, *Acta Metall. Mater*. **18** (1990) 1933–1940.
[4] U. Essmann, U. Gosele, H. Mughrabi, *Phil. Mag. A* **44** (1981) 405–426.
[5] C. Blochwitz, *Mater. Sci. Eng.* A141 (1991) 49–51.
[6] Berfield, T. A., Patel, J. K., Shimmin, R. G., Braun, P. V., Lambros, J., and Sottos, N. R. *Expl Mechanics* 47(2007) 51–62.
[7] Scrivens, W. A., Luo, Y., Sutton, M. A., Collette, S.A., Myrick, M. L., Miney, P., Colavita, P. E., Reynolds, A. P., and Li, X. *Expl Mechanics* 47(1) 2007 63–77.
[8] Knauss,W. G., Chasiotis, I., and Huang, Y, *Mechanics of Mater*, 35 (2003) 217–231.
[9] Sutton, M. A., Li, N., Joy, D. C., Reynolds, A. P., Li X., *Expl Mechanics*, **47** (2007) 775–787.
[10] S. Avril, P. Feissel, F. Pierron, P. Villon. *Measurement Science & Technology, IOP Publishing Ltd*, 21.1, 015703 2010.
[11] B. Nayroles, G. Touzot, P. Villon. La méthode des éléments diffus. Comptes rendus de l’Académie des Sciences, série 2, Mécanique, Physique, Chimie, Sciences de l’Univers, Sciences de la Terre, 313-2, 133 138, 1991.